Simulated Space Environment Effects on a Candidate Solar Sail Material

By Jin Ho KANG[1)], Robert G. BRYANT[2)], W. Keats WILKIE[2)], Heather M. WADSWORTH[3)], Paul D. CRAVEN[4)], Mary K. NEHLS[4)] and Jason A. VAUGHN[4)]

[1)]*National Institute of Aerospace, Hampton, VA, USA*
[2)]*National Aeronautics and Space Administration Langley Research Center, Hampton, VA, USA*
[3)]*Virginia Polytechnic Institute and State University, Blacksburg, VA, USA*
[4)]*National Aeronautics and Space Administration Marshall Flight Space Center, Huntsville, VA, USA*

(Received 1st Dec, 2016)

For long duration missions of solar sails, the sail material needs to survive harsh space environments and the degradation of the sail material controls operational lifetime. Therefore, understanding the effects of the space environment on the sail membrane is essential for mission success. In this study, we investigated the effect of simulated space environment effects of ionizing radiation, thermal aging and simulated potential damage on mechanical, thermal and optical properties of a commercial off the shelf (COTS) polyester solar sail membrane to assess the degradation mechanisms on a feasible solar sail. The solar sail membrane was exposed to high energy electrons (about 70 keV and 10 nA/cm^2), and the physical properties were characterized. After about 8.3 Grad dose, the tensile modulus, tensile strength and failure strain of the sail membrane decreased by about 20 ~ 95%. The aluminum reflective layer was damaged and partially delaminated but it did not show any significant change in solar absorbance or thermal emittance. The effect on mechanical properties of a pre-cracked sample, simulating potential impact damage of the sail membrane, as well as thermal aging effects on metallized PEN (polyethylene naphthalate) film will be discussed.

Key Words: Solar sail membrane, Polyethylene Naphthalate, Space Environment, Degradation, Radiation

Nomenclature

χ_c	:	crystallinity
H_f	:	heat of fusion
w_f	:	specific total work of fracture
w_e	:	specific essential work to fracture
w_p	:	non-essential work (plastic deformation)

1. Introduction

Solar sails are attractive spacecraft propulsion systems that offer extended mission capability by deriving thrust directly from momentum transfer of solar photons, rather than onboard fuel.[1-2)] The transferred photon momentum is very small but the acceleration can be maximized by increasing the surface area of the sail. For long duration missions, the sail material needs to survive temperature fluctuations, ultraviolet (UV) rays, ionizing radiation, ultrahigh vacuum, and micrometeoroid impacts.[3-7)] Since the degradation of the sail material controls operational lifetime, understanding the effects of the space environment on the sail membrane is essential for mission success.

There have been several studies of space environment effects on candidate sail materials such as aluminized Mylar™ (polyethylene terephthalate, PET), Teonex™ (polyethylene naphthalate, PEN), CP1™ (colorless polyimide) and Kapton™ polyimide.[5-7)] After exposure of high energy electrons, protons and UV rays, the degradation of physical properties of sail materials was demonstrated. However, there is no systematic study to investigate the chemical changes induced in the polymer under simulated space environment exposure.

In this study, we simulated the effect of the space environment of ionizing radiation, thermal aging and impact damage on mechanical, thermal, and optical properties of a commercial off the shelf (COTS) polyester membrane to assess the degradation mechanisms on a feasible solar sail. A quantitative study of space environment effects on the solar sail can provide design guidelines to increase the reliability of solar sails, resulting in increased acceptance of this type of propulsion system.

2. Experimental

2.1. Materials

PEN (Figure 1) as a sail core membrane was purchased from Dupont Teijin (Teonex™ Q72, 2μm thick). Metallized PEN was prepared by deposition of aluminum (1000Å) on the front side of the membrane as a reflective layer and chromium (150Å) on the back side of the membrane as a thermal emitter, respectively (Astral Technology Unlimited, Inc.).

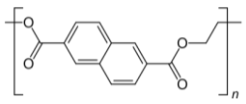

Fig. 1. Molecular structure of PEN.

2.2. Electron Irradiation Test

Electron irradiation tests were performed by the Space Environmental group at NASA Marshall Space Flight Center (MSFC). The metallized PEN film was exposed to electron radiation for nineteen days with a fluence of 1.04x10^{17}

electrons/cm^2. The electron beam energy and current were 70keV and 10 nA/cm^2, respectively. The total exposure dosage was approximately 8.3 Grad. A Hitachi S-5000 high-resolution scanning electron microscope (HSEM), with a field emission electron gun and in-lens detector was used to examine the surface morphology of the metallized PEN film. Infrared (IR) spectra were taken in transmission mode with a Fourier Transform Infrared (FT-IR) spectrometer (Nicolet iS^{TM} 5).

2.3. Thermal Analysis

Viscoelastic behavior of the metallized PEN film was characterized from storage and loss modulus at a heating rate of 1°C/min and 1 Hz in a dynamic mechanical analyzer (DMA Q800, TA Instruments). Thermal properties of melting, crystalline and glass transition temperature of the metallized PEN film were characterized at a heating rate of 3°C/min with a modulation of ±0.47°C for every 60 seconds using a modulated differential scanning calorimeter (MDSC, Q2000, TA Instruments). Coefficient of thermal expansion (CTE) was determined from the dimension change at a heating rate of 5°C/min in a thermomechanical analyzer (TMA, model 202, Netzsch.

2.4. Thermal Aging Test

The metallized PEN film was exposed to elevated temperatures, and the mechanical and optical properties were measured. The films were affixed to glass slides to prepare for treatment at temperatures ranging from 75 to 275°C. The specimens were placed in a nitrogen purged convention oven (Blue M) and held at the treatment soak temperature for ten minutes. The treated specimens were examined under an optical microscope in reflectance and transmittance mode to examine cracking. Ultraviolet-visible-infrared (UV-VIS-IR) spectroscopy (PerkinElmer, Lambda 1050 spectrometer) was performed in reflectance mode to determine the reflectivity from 250 to 2400 nm at room temperature.

2.5. Mechanical Property Test

Tensile properties of film were characterized according to ASTM standard D882-12.[8] Specimens (about 5 mm wide) were placed between grips with a gauge length of about 50 mm and pulled at a rate of 5 mm/minute until failure.

Mode I tearing test was performed to calculate the essential work of fracture (EWF). Samples were prepared by cutting along the two directions [machine direction (MD) and transverse direction (TD) of a film roll] to see the effect of cutting direction. Double-edge notched tension (DENT) specimens 20 mm wide with 2, 4, 6, 8, and 10 mm ligament lengths were prepared using a straightedge and razor blade. The specimens were gripped with an initial gauge length of 40 mm and pulled at a rate of 0.1 mm/minute until failure. The setup for this test is shown in Figure 2. Load-displacement graphs were generated and the essential work of fracture calculated.

Tear-propagation resistance in Mode III for the metallized PEN film was evaluated using ASTM standard D1938-14.[9] Trouser-shaped specimens 25 mm wide and 75 mm long with a vertical pre-crack of 50 mm were prepared using a straightedge and razor blade. The specimen was gripped at the two panels created by the crack with an initial grip separation of 50 mm. The top grip was extended at a rate of 250 mm/minute until the tear propagated through the entire length of the specimen, and load-displacement plots were generated. The setup for this test is shown in Figure 3.

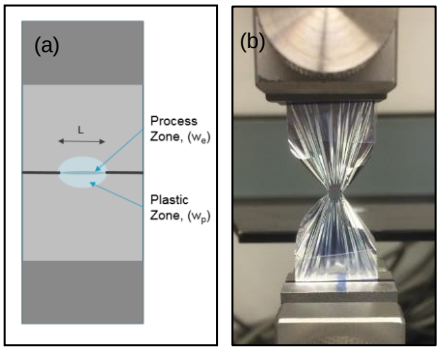

Fig. 2. (a) Sample preparation and (b) setup during testing for DENT configuration (Mode I tear test).

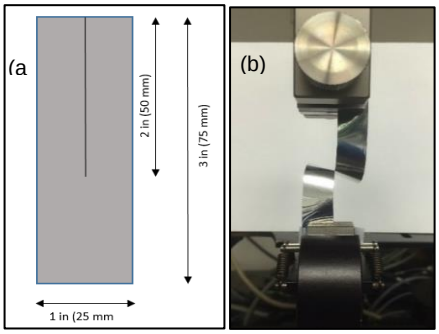

Fig. 3. (a) Sample configuration and (b) setup during testing for Mode III tear-propagation resistance.

To simulate potential impact damage on the sail membrane, holes and slits were introduced before tensile testing of the metallized PEN film. Specimens 20 mm wide with a gauge length of 100 mm were prepared. The pre-cracks of 2 mm width were made with a razor blade and a 2 mm diameter circular die (Figure 4). Tensile testing was performed with an extension rate of 5 mm/minute and load-displacement graphs generated.

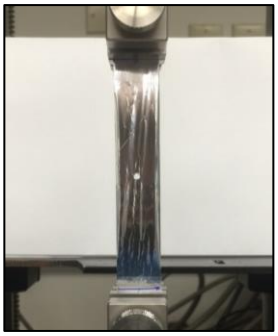

Fig. 4. Setup for tensile test of metallized PEN film with a 2 mm die-cut hole to simulate potential impact damage.

3. Results

3.1. Electron irradiation

Figure 5 shows the appearance change of the metallized PEN film after electron irradiation of approximately 8.3 Grad. The irradiated film became wrinkled. This seemed to be originated from induced stress and thermal energy by electron radiation.

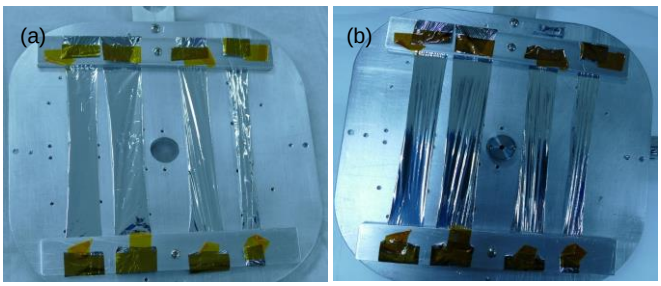

Fig. 5. Metallized PEN film on the sample holder plate (a) before electron irradiation and (b) after electron irradiation.

The surface morphology of the film was investigated by a scanning electron microscopy (SEM) (Figure 6). Before irradiation, the film showed a smooth aluminum layer. However, after electron irradiation, the aluminum coating was damaged and delaminated exposing the PEN core layer underneath [Figure 6 (b)]. Even though the surface of aluminum coating was damaged, the solar absorbance of the aluminum side was unchanged (0.09 for control PEN film, and 0.09 for electron irradiated PEN film, Table 1). The thermal emittance of the aluminum side of the PEN film slightly increased from 0.05 for control PEN to 0.09 for irradiated PEN.

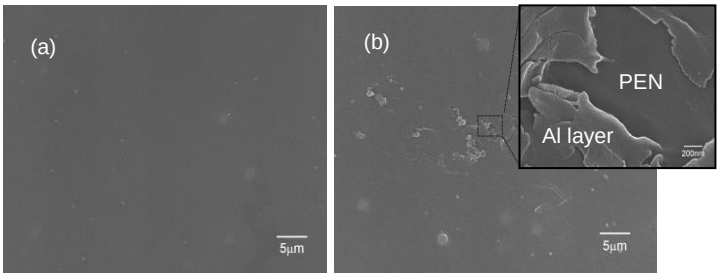

Fig. 6. SEM image of the aluminum coating surface of the metallized PEN film (a) before electron irradiation and (b) after electron irradiation.

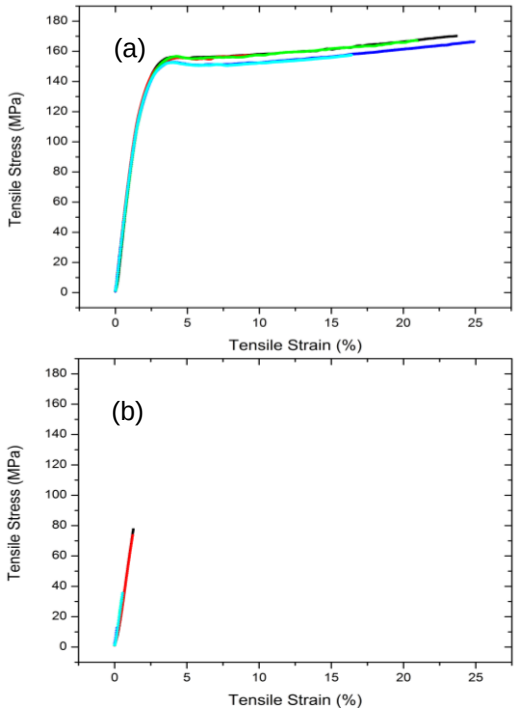

Fig. 7. Tensile properties of metalized (a) control PEN and (b) electron irradiated PEN film. Each color represents one of 5 tensile test specimens.

Electron radiation exposure of the metallized PEN film led to a decrease in mechanical properties when compared to the control specimens, as shown in Figure 7 and Table 1. The change was obvious even before testing began because the samples were very brittle, and difficult to handle and set up for testing. The elastic modulus of the PEN dropped from 8.43 GPa to 6.56 GPa, and the exposed specimens broke near one percent elongation, indicating substantial embrittlement. The tensile strength was reduced from approximately 165 MPa to 46 MPa. The degradation of mechanical properties could be explained by chain scission and crosslinking of polymer molecules from high energy electron radiation.

Table 1. Physical properties of the metallized PEN

Metalized Film	Modulus (GPa)	Tensile Strength (MPa)	Elongation at break (%)	Solar Absorbance	Thermal Emittance
Control PEN	8.43 ± 0.14	164.89 ± 5.35	18.20 ± 5.97	0.09	0.05
Electron irradiated PEN	6.56 ± 0.23	46.42 ± 25.09	0.76 ± 0.44	0.09	0.09

The electron radiation induced molecular degradation was observed using various experimental techniques. Figure 8 shows storage and loss modulus of metallized PEN film as a function of temperature. The storage modulus of the control PEN film was about 5 – 9 GPa in the range of -60°C to 120°C. Above the glass transition (α-transition) of about 140°C, the storage modulus decreased and was about 1.3 GPa just before melting (near 270°C). After electron irradiation, both the overall storage modulus and the glass transition decreased (from 140°C to 137°C). The most interesting observation is significant increase in a loss modulus at β^*-transition, representing the out-of-plane motions of naphthalene rings or the fluctuation of aggregates of naphthalene rings.[10] The ratio of loss modulus of α-transition and β^*-transition for the electron irradiated PEN film decreased to 0.62 from the 1.19 for the control PEN film, which indicates an increase in the short segmental mobility induced from chain scission of main polymer chains by high energy radiation. The chain scission was also established from the differential scanning calorimetry (DSC) thermogram (Figure 9) and FT-IR spectra (Figure 10). The control PEN film shows a clear melting peak at about 260°C with 1st heating run and high crystallinity (χ_c) of about 54%, determined by

$$\chi^c = \Delta H_f(m)/\Delta H_f(c) \quad (1)$$

where $\Delta H_f(m)$ is the measured heat of fusion of the semicrystalline PEN and $\Delta H_f(c)$ is the heat of fusion of 100% crystalline PEN (103J/g).[11] With the second heating run, it showed a clear glass transition (at about 124°C), a crystalline peak (at about 190°C) and melting peak (at about 260°C), in that order. On the contrary, the electron irradiated PEN film showed neither a clear glass transition nor a crystalline peak while showing a broad and small melting peak with the first heating run (χ_c of about 9%), which represents molecular chain degradation.

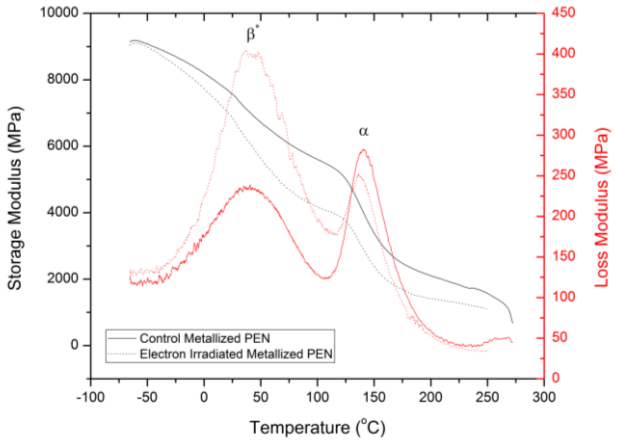

Fig. 8. DMA curves of control and electron irradiated PEN film.

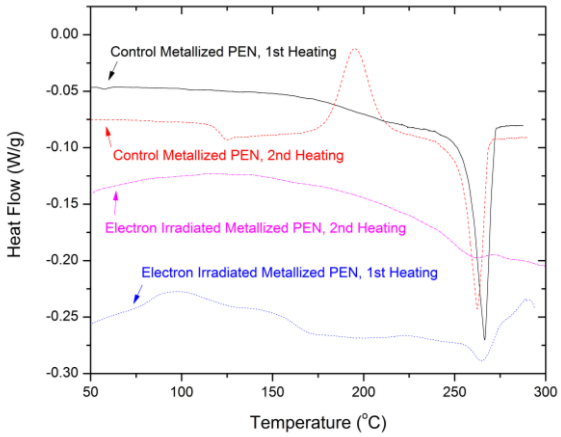

Fig. 9. DSC curves of control and electron irradiated PEN film.

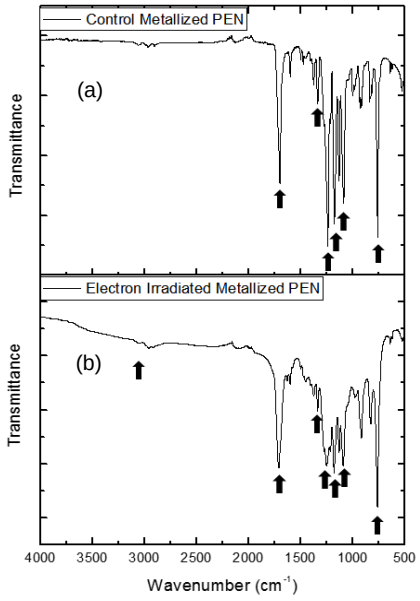

Fig. 10. FT-IR spectra of (a) control and (b) electron irradiated PEN film.

Figure 10 shows the change of molecular structure of metallized PEN film after electron irradiation. Compared to the peak for CH out of plane of aromatic moiety (760cm^{-1}), the peaks of =C-O (1240cm^{-1}), C-O-C (1178cm^{-1}), -O-C (1085cm^{-1}) and CH_2 (1374, 1339cm^{-1}) of esters appear less intense, and apparent carboxylic acid characteristic peaks (the broad peak of -OH at about 3000cm^{-1} and C=O at 1700cm^{-1}) begin to appear. This suggests that the PEN molecules were decomposed to some degree by electron irradiation to yield carboxylic acid moieties (naphthanoic end groups).

3.2. Thermal Aging Test

Thermal aging of metallized PEN film was examined. Figure 11 shows the coefficient of thermal expansion (CTE) of raw PEN film (without metal coatings) and metallized PEN film as a function of temperature. The CTE of the samples varied from about 9 to 13 ppm/°C for the range of 0 ~ 100°C. While the raw PEN films showed a large increase in CTE above the glass transition temperature (around 124°C), the metallized PEN films maintained a low CTE until reaching the melting temperature (about 260°C) because the metallic layers can restrict the macroscopic dimension change of PEN film. This represents that the operational limit of the metallized PEN film is more a function of the melting temperature, than the glass transition temperature.

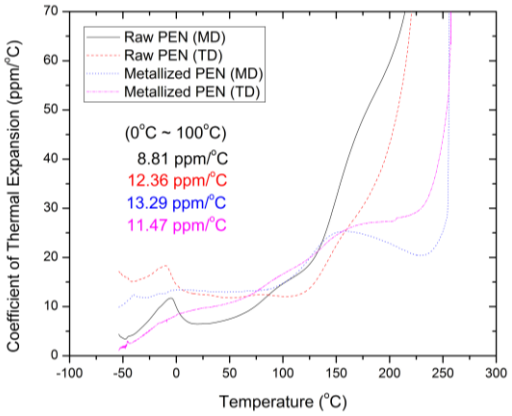

Fig. 11. CTE of raw PEN film and metallized PEN film.

The appearance changes of the metallized PEN film after thermal treatment at various temperatures are shown in Figure 12. The PEN film was dimensionally stable up to about 150°C.

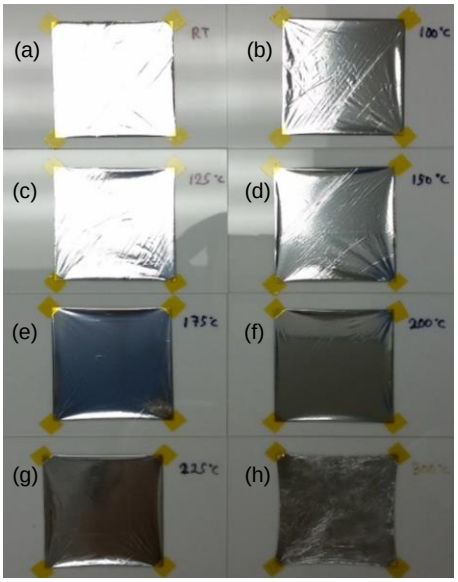

Fig. 12. Appearance of metallized PEN film after thermal aging test at (a) room temperature, (b) 100°C, (c) 125°C, (d) 150°C, (e) 175°C, (f) 200°C, (g) 225°C and (h) 300°C.

Above 150°C, there was some noticeable shrinkage below the melting temperature (around 260°C). The sample aged at 300°C, [Figure 12. (h)] resulted in a significant degree of distortion. Cracks on the surfaces were observed by an optical microscope.

Figure 13 shows spectral reflectance of metallized PEN films after thermal aging. The thermally aged metallized PEN films did not exhibit any significant change in reflectance, while the sample treated at 300°C showed a slight decrease in reflectance resulting from thermal distortion leading to surface cracks.

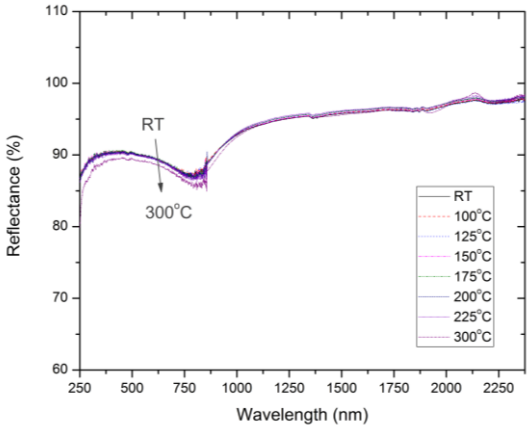

Fig. 13. Spectra reflectance of metallized PEN film after thermal aging at various temperatures from RT to 300°C.

The mechanical properties of metallized PEN film after thermal treatment are shown in Figure 14. The modulus and tensile strength of thermally aged samples slightly decreased within experimental error, while the elongation at the break of the sample treated at 225°C showed significant reduction. This would indicate that the metallized PEN sustains the stable mechanical properties after thermal aging at about 200°C.

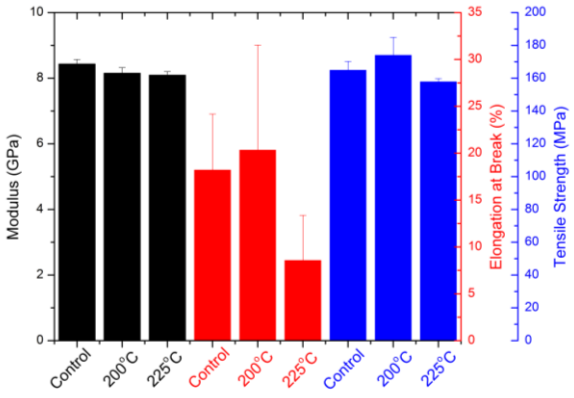

Fig. 14. Mechanical properties of metallized PEN film after thermal aging at various temperatures of room temperature (control), 200 and 225°C.

3.3. Simulated impact damage on mechanical properties

The primary cause of concern from micrometeoroid is physical damage upon impact. Erosion of surface materials can change spectral reflectance of sail membrane.[3] Even catastrophic failure can result from strain propagated tearing created from impact damage. Thus, tearing properties of a sail membrane as a function of damage geometry should be studied. Mode I tearing fracture of metallized PEN film was examined using the EWF method to separate the essential work to fracture the polymer (w_e) from the non-essential geometry-dependent work from plastic deformation (w_p)[12-13]

$$w_f = w_e + \beta w_p L \quad (2)$$

where w_f is the specific total work of fracture and β is proportionality constant (plastic zone shape factor) whose value depends on the geometry of the specimen and the crack.

Tensile tests of the DENT specimens with various ligament lengths (Figure 2) were plotted in Figure 15 (a). The load-extension plot shows that the maximum load and extension before failure decreases as the ligament length decreases, while the shape of the plots for varying ligament lengths remains the same. From the load-extension graph, the total work of fracture was calculated to obtain the w_e and β [Figure 15 (b) and Table 2]. w_e of metallized PEN films were 23.8 and 27.3 kJ/m^2 for MD and TD, respectively. These measured values are lower than the literature stated range of 55 – 75 kJ/m^2, probably because the metallized PEN was manufactured by bi-axially stretching to induce high crystallinity (over 50%). Also, the bubbles in the film, which were discovered using microscopy, can lower fracture toughness. β, which represents geometry related plastic zone factor was less than literature value (5 – 23 MJ/m^3).

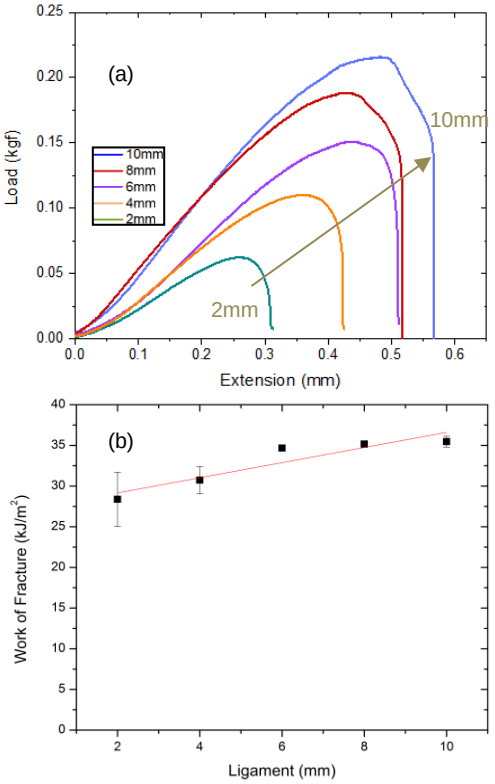

Fig. 15. Mode I tear fracture property of metallized PEN film. (a) Load vs. displacement profile and (b) specific total work of fracture (w_f) vs. ligament length (L).

Mode III tearing fracture toughness was measured by a trouser tear test (Figure 3). The trouser tear specimen was gripped at the two panels created by the pre-crack and the load was recorded with crack propagation induced by the extension of a grip distance. The approximate load of 1.5 mN for the

metallized PEN was required for the pre-crack to propagate, which shows that the material can fail catastrophically under a light load if an edge crack is present. Tearing energy and work are summarized in Table 2.

Table 2. Tear Physical properties of the metallized PEN

Material		Mode I tear fracture		Mode III tear fracture	
		Essential work of fracture, w_e (kJ/m^2)	Shape factor, β (kJ/m^3)	Tearing energy (N/m)	Tearing work (N·m)
Metallized PEN	MD	23.8 ± 1.5	1.1 ±0.2	1361.0 ± 58.9	72.0 ± 3.1
	TD	27.3 ± 1.4	0.9 ±0.2	1517.4 ± 179.2	80.2 ± 9.5

To investigate the impact damage on the mechanical property, holes and slits were introduced into the membrane. Metallized PEN film with pre-cracks from die (2 mm diameter die hole) and blade cuts (2 mm wide slit) failed at a lower load and elongation than control specimens. The 2 mm diameter die cut specimens failed at a tensile stress and strain of approximately 130 MPa and 2.5%. The specimens with 2 mm wide slit failed at approximately 60 MPa and 1% elongation. Even though the pre-damage was introduced, the induced tensile stress is higher than the biaxial tension level of deployed solar sails (about 0.007 MPa (about 1 psi)).[14)]

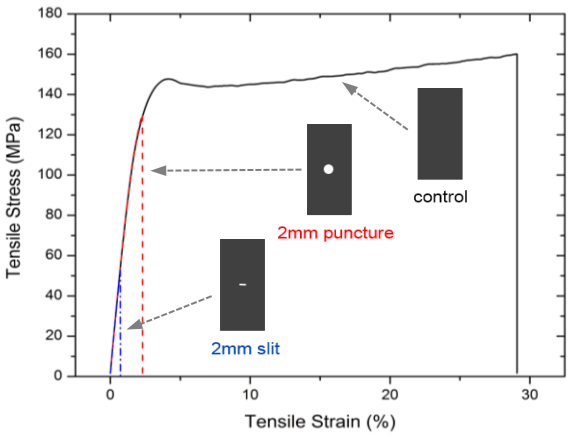

Fig. 16. Tensile property of metallized PEN film with simulated impact damage.

4. Conclusion

The effects of select simulated space environments on mechanical, thermal and optical properties of a COTS polyester, metallized PEN solar sail membrane were investigated by electron irradiation, thermal aging and simulated impact damage test. After about 8.3 Grad dose of electron irradiation, the tensile modulus, tensile strength and failure strain of metallized PEN film decreased by about 20 ~ 95%. However, it did not show any significant change in optical properties of solar absorbance and thermal emittance of the reflective side (aluminum layer). By thermal and spectroscopic analysis, polymer molecular degradation under electron irradiation was confirmed. From the thermal aging tests, it is speculated that the operational temperature limit of metallized PEN sail can be assumed to approach the melting temperature of PEN, with the elongation result from the thermal aging being a better predictor. The pre-cracked specimens to simulate potential impact damage exhibited significant degradation in tensile strength. The further quantitative study of space environment effects such as proton, UV radiation or combined radiation on the solar sail membrane can provide design guidelines to increase the reliability of solar sails.

Acknowledgments

Authors acknowledge Drs. Sheila Thibeault and D. Laurence Thomsen III for their valuable comments on radiation effects, and Mr. Harold Claytor, Mr. Joel Alexa and Ms. Crystal Chamberlain for their help in experimental preparation.

References

1) Wilkie, W. K., Warren, J. E., Thompson, M. W., Lisman, P. D., Walkemeyer, P. E., Guerrant, D. V. and Lawrence, D. A.: The Heliogyro Reloaded, Joint Army-Navy-NASA-Air Force (JANNAF) Interagency Propulsion Committee Meeting, Huntsville, AL, USA, December 5-9, 2011.
2) Mcinnes, C. R.: *Solar Sailing: Technology, Dynamics and Mission Application*, Springer Praxis, New York, 1999.
3) Tribble, A. C.: *The Space Environment: Implications for Spacecraft Design*, Princeton University Press, New Jersey, 2003.
4) Bryant, R. G., Seaman, S. T., Wilkie, W. K., Miyauchi, M. and Working, D. C.: Selection and Manufacturing of Membrane Materials for Solar Sails, *Advances in Solar Sailing*, *Macdonald, M. (ed.).*; Springer Berlin Heidelberg, 2014; pp 525-540.
5) Edwards, D. L., Semmel, C., Hovater, M., Nehls, M., Gray, P. Hubbs, W. and Werts, G.: Solar Sail Material Performance Property Response to Space Environmental Effects, *Proceedings of SPIE*, Vol 5554, SPIE, Bellingham, WA, 2004.
6) Edwards, D. L., Hubbs, W. S., Wertz, G. E., Hoppe, D. T., Nehls, M. K., Hollerman,W. A., Gray, P. A. and Semmel, C. L.: Electron Radiation Effects on Candidate Solar Sail Material, *High Performance Polymers*, 16 (2003), pp.277-288.
7) Hollerman, W., Bergeron, N. P. and Moore, R. J.: Proton Survivability Measurements for Candidate Solar Sail Materials, *IEEE Nuclear Science Symposium Conference Record*, 2005, pp. 1436-1440.
8) ASTM Standard D882-12, "Standard Test Method for Tensile Properties of Thin Plastic Sheeting."
9) ASTM Standard D1938-14, "Standard Test Method for Tear-Propagation Resistance of Plastic Film and Thin Sheeting by a Single-Tear Method."
10) Hardy, L., Stevenson, I., Fritz, A., Boiteux, G., Seytre, G. and Schönhals, A.: Dielectric and Dynamic Mechanical Relaxation Behavior of Poly(ethylene 2,6-naphthalate dicarboxylate). II. Semicrystalline Oriented Films, *Polymer*, 44 (2003), pp. 4311-4323.
11) Wunderlich, B. and Cheng, S. Z. D.: Glass Transition and Melting Behavior of Poly(ethylene-2,6-naphthalenedicarboxylate), *Macromolecules*, **21** (1988), pp. 789-797.
12) Bárány, T., Czigány, T. and Karger-Kocsis, J. Application of the Essential Work of Fracture (EWF) Concept for Polymers, Related Blends and Composites: A Review, *Progress in Polymer Science*, **35** (2010), pp. 1257-1287.
13) Arkhireyeva, S. and Hashemi, S.: Fracture Behaviour of Polyethylene naphthalate (PEN), *Polymer*, **43** (2002), pp.289-300.
14) Greschik, G. and Mikulas, M. M.: Design Study of a Square Solar Sail Architecture, *Journal of Spacecraft and Rockets*, **39** (2002), pp. 653-661.